Available online at www.sciencedirect.com

ScienceDirect

Procedia Engineering 64 (2013) 661 – 670

Procedia Engineering

www.elsevier.com/locate/procedia

International Conference On DESIGN AND MANUFACTURING, IConDM 2013

Numerical Simulation of Plane Crack Problems using Extended Isogeometric Analysis

G. Bhardwaj, I. V. Singh*, B. K. Mishra

Department of Mechanical and Industrial Engineering, Indian Institute of Technology Roorkee, Roorkee, U.K., India,

Abstract

This paper presents the simulation of plane crack problems using extended isogeometric analysis (XIGA). In XIGA, both geometry and solution are approximated using NURBS basis functions. Discontinuous Heaviside function is used to model the crack face, while crack tip singularity is modeled using asymptotic crack tip enrichment functions. Few plane crack problems are solved in the presence of multiple holes and inclusions using XIGA. These simulations show that the SIFs obtained using XIGA gives more accurate results as compared to those obtained by XFEM.

Keywords: Edge crack; NURBS; Extended isogeometric analysis (XIGA); Discontinuities; Enrichment functions.

1. Introduction

Now a day, the most of the engineering problems are solved using FEM. It suffers from the disadvantage of

Nomenclature

Ξ	knot vector
p	order of polynomial
n	Number of basis function

* Corresponding author. Tel.: +91-1332-285888; fax: +91-1332-285665.
E-mail address: ivsingh@gmail.com

doi:10.1016/j.proeng.2013.09.141

R	NURBS basis function
N	B-spline basis function

conformal meshing for solving fracture problems. In past, the fracture analysis of structures is presented by the combination of isogeometric analysis (IGA) and XFEM. In IGA [1], non-uniform rational B-splines (NURBS) basis functions are used for the representation of the geometries as well as the solution. So far, the IGA have been successfully implemented in various fields such as gradient damage modeling [2], cohesive zone modeling [3] and topology optimization [4] and many more. The implementation of NURBS based IGA for contact problems [5] gives greater accuracy and faster convergence rate as compared to the Lagrange finite elements. Nearly same accuracy is achieved using NURBS based IGA with fewer degrees of freedom in fracture mechanics problems [6-7]. The different problems of stationary as well as propagating crack [8] are solved using extended isogeometric analysis (XIGA). The bi-material body with a curved interface [9] is analyzed by combination of quadratic NURBS basis function and XFEM.

In the present work, XIGA is used for the simulation of planer crack problems. A plane edge crack problem is solved using first, second and third order NURBS basis functions. Two edge crack problems are solved in the presence of multiple holes and inclusions. The values of stress intensity factors (SIFs) are computed using domain based interaction integral approach.

2. Isogeometric Analysis

2.1. Basis Function

The knot vector, B-spline functions and NURBS functions are discussed in this section. B-splines are built from piecewise polynomial functions. The details of NURBS can be found in Ref. [10]. The knot vector Ξ is defined by a set of coordinates, or knots, which gives information where the subintervals are connected. $\Xi = \{\xi_1, \xi_2, ...\xi_{n+p+1}\}$ are the real coordinates represent the geometry in parametric space [0,1], where ξ_i is the i^{th} knot, i is the knot index, $i = 1, 2... n+p+1$, p is polynomial order and n is number of basis function used to construct the B-spline curve.

In the isogeometric analysis, different types of knot vectors are used: open knot vector and closed knot vector. In the present analysis, open knot vector is used, where end knots are repeated $p+1$ times. B-spline basis are defined recursively starting with $p=0$ in the following manner [10].

$$N_{i,0} = \begin{cases} 1 & \xi_i \le \xi \le \xi_{i+1} \\ 0 & otherwise \end{cases}, \quad N_{i,k}(\xi) = \frac{\xi - \xi_i}{\xi_{i+k-1} - \xi_i} N_{i,k-1}(\xi) + \frac{\xi_{i+k} - \xi}{\xi_{i+k} - \xi_{i+1}} N_{i+1,k-1}(\xi) \tag{1}$$

The derivatives of B-spline basis function can be calculated for a given order of polynomial and knot vector:

$$\frac{dN_{i,p}(\xi)}{d\xi} = \frac{p}{\xi_{i+p} - \xi_i} N_{i,p-1}(\xi) - \frac{p}{\xi_{i+p+1} - \xi_{i+1}} N_{i+1,p-1}(\xi) \tag{2}$$

A rational B-spline curve defined by $n+1$ control points B_i is given by [10]:

$$P(\xi) = \sum_{i=0}^{n} B_i R_{i,p}(\xi), \quad R_{i,p}(\xi) = \frac{w_i N_{i,p}(\xi)}{W(\xi)} = \frac{w_i N_{i,p}(\xi)}{\sum_{i=0}^{n} w_i N_{i,p}(\xi)} \tag{3}$$

where, $R_{i,p}(\xi)$ are the NURBS basis function, B_i are the coordinates of control point (X_i, Y_i), w_i are the weights associated with the control points, and $N_{i,p}(\xi)$ are the *B*-spline basis function of order *p* defined using knot vector.

The length of the knot vector is given as [11]. $m = n + p + 1$ (4)

The derivative of NURBS basis function can be computed as

$$\frac{dR_{i,p}(\xi)}{d\xi} = w_i \frac{W(\xi)N'_{i,p}(\xi) - W'(\xi)N_{i,p}(\xi)}{(W(\xi))^2} \tag{5}$$

NURBS has the following features

- NURBS basis function forms a partition of unity $\sum_{i=1}^{n} R_{i,p}(\xi) = 1$.
- The support of each $R_{i,p}(\xi)$ is compact and contained in interval $[\xi_i, \xi_{i+p+1}]$.
- NURBS insure $p-1$ continuous derivatives if internal knots are not repeated, whereas it produces C^{p-k} continuity if knot has multiplicity k .

2.2. Isogeometric Discretization:

A given domain is partitioned into displacement Γ_u , traction Γ_t and traction free boundaries Γ_c . The equilibrium equation and boundary conditions are defined as [12]

$$\nabla.\boldsymbol{\sigma} + \mathbf{b} = \mathbf{0} \text{ in } \Omega, \quad \sigma.\hat{n} = \overline{t} \quad on \ \Gamma_t, \ \sigma.\overline{n} = 0 \quad \text{on } \Gamma_c \tag{6}$$

where, $\boldsymbol{\sigma}$ is Cauchy stress tensor and $\mathbf{b}$ is body force per unit volume.

The constitutive relation for the elastic material under consideration is given by Hook's law:

$$\boldsymbol{\sigma} = D\varepsilon \tag{7}$$

A weak form of the equilibrium equation [13] is given as:

$$\int_{\Omega} \boldsymbol{\sigma}(\mathbf{u}) : \boldsymbol{\varepsilon}(\mathbf{v}) d\Omega = \int_{\Omega} \mathbf{b}.\mathbf{v} d\Omega + \int_{\Gamma_t} \overline{\mathbf{t}}.\mathbf{v} d\Gamma \tag{8}$$

On substituting the trial and test functions and using the arbitrariness of nodal variations, the following discrete system of equations are obtained

$$[\mathbf{K}]\{\mathbf{d}\} = \{\mathbf{f}\} \tag{9}$$

where, $\mathbf{K}$ is the global stiffness matrix, $\mathbf{d}$ is the vector of nodal unknowns and $\mathbf{f}$ is the external force vector. B matrix of basis function derivatives is given by [8]:

$$B = \begin{bmatrix} \frac{\partial R_1}{\partial X_1} & 0 & ..... & \frac{\partial Rn_{en}}{\partial X_1} & 0 \\ 0 & \frac{\partial R_1}{\partial X_2} & ..... & 0 & \frac{\partial Rn_{en}}{\partial X_2} \\ \frac{\partial R_1}{\partial X_2} & \frac{\partial R_1}{\partial X_1} & ..... & \frac{\partial Rn_{en}}{\partial X_2} & \frac{\partial Rn_{en}}{\partial X_1} \end{bmatrix} \tag{10}$$

where, $R(\xi)$ is a vector of NURBS basis functions, R_i ($i = 1,2,.....n_{en}$) in the parametric space of $\xi = (\xi_1, \xi_2)$. $n_{en} = (p+1)\times(q+1)$ are the number of non-zero basis function for a given knot span i.e. element, where, p and q are the order of curve in ξ_1 and ξ_2 directions respectively. The physical coordinates $X = (X_1, X_2)$ and displacement approximation u^h can be derived for a particular point $\xi = (\xi_1, \xi_2)$ i.e. parametric coordinate.

$$u^h(\xi) = \sum_{i=1}^{n_{en}} R_i(\xi) u_i, \quad X(\xi) = \sum_{i=1}^{n_{en}} R_i(\xi) B_i \tag{11}$$

3. **Extended Isogeometric Analysis**

In extended isogeometric analysis, the displacement approximation is locally enriched to simulate discontinuities. Few degrees of freedom are added to the selected control points near the location of a crack.

3.1. XIGA approximations for cracks

In XIGA, for modeling crack edge and tip, Equation (11) can be written in generalized form as

$$u^h(\xi) = \sum_{i=1}^{n_{en}} R_i(\xi) u_i + \sum_{j=1}^{n_{cf}} R_j(\xi) H(\xi) a_j + \sum_{k=1}^{n_{ct}} R_k(\xi) (\sum_{\alpha=1}^{4} \beta_\alpha(\xi) b_k^\alpha) \tag{12}$$

where $H(\xi)$ and β_α are the Heaviside function and crack tip enrichment functions respectively. The additional degrees of freedom related to the modeling of crack face and crack tip are represented by vectors a_j and b_k^α respectively. The n_{cf} is the number of n_{en} basis function that have crack face in their support domain and n_{ct} is the number of basis function associated with crack tip in the domain of influence. Heaviside function $H(\xi)$ is +1 (if physical coordinates corresponding to parametric coordinates ξ) is above crack and -1 on the other side of discontinuity. The crack tip enrichment functions are defined as [12]:

$$\beta_\alpha(\xi) = [\sqrt{r}\cos\frac{\theta}{2}, \sqrt{r}\sin\frac{\theta}{2}, \sqrt{r}\cos\frac{\theta}{2}\sin\theta, \sqrt{r}\sin\frac{\theta}{2}\sin\theta\ ]$$

where, r and θ are the local crack tip parameters.

3.2. XIGA approximations for hole

The XIGA approximation for holes can be written as:

$$u^h(\xi) = \sum_{i=1}^{n_{en}} R_i(\xi) u_i + \sum_{j=1}^{nc_f} R_j(\xi) \chi(\xi) c_j \tag{13}$$

where, c_j is the nodal enriched degree of freedom associated with Heaviside function $\chi(\xi)$ which takes a value +1 for the nodes lying outside and 0 for inside the hole.

3.3. XIGA approximation for Inclusion

The XIGA approximation for inclusions can be written as

$$u^h(\xi) = \sum_{i=1}^{n_{en}} R_i(\xi) u_i + \sum_{j=1}^{n_{en}} R_j(\xi)\psi(\xi) d_j \tag{14}$$

where, $\psi(\xi)$ and d_j are corresponds to the level set function and degree of freedom associated with level set function.

3.4. XIGA formulation for a crack

The first term in the right hand side of "Eq. (12)" evaluates the displacement field by using classical IGA approximation, while the remaining terms are enrichment approximation to model discontinuity and to represent solution accurately near the crack tip. The elemental matrices $\mathbf{K}$ and $\mathbf{f}$ in "Eq. (9)", are obtained using the approximation function defined in "Eq. (11)".

$$\mathbf{K}_{ij}^{e} = \begin{bmatrix} K_{ij}^{uu} & K_{ij}^{ua} & K_{ij}^{ub} & K_{ij}^{uc} & K_{ij}^{ud} \\ K_{ij}^{au} & K_{ij}^{aa} & K_{ij}^{ab} & K_{ij}^{ac} & K_{ij}^{ad} \\ K_{ij}^{bu} & K_{ij}^{ba} & K_{ij}^{bb} & K_{ij}^{bc} & K_{ij}^{bd} \\ K_{ij}^{cu} & K_{ij}^{ca} & K_{ij}^{cb} & K_{ij}^{cc} & K_{ij}^{cd} \\ K_{ij}^{du} & K_{ij}^{da} & K_{ij}^{db} & K_{ij}^{dc} & K_{ij}^{dd} \end{bmatrix}, \quad (i, j = 1,2,3.....n_{en}) \tag{15}$$

The discretized form of governing equation:

$$\mathbf{K}_{ij}^{rs} = \int_{\Omega^e} (\mathrm{B}_i^r)^T \mathbf{C}\, \mathrm{B}_j^s \, h d\Omega, \quad where \quad r,s = u,a,b,c,d \tag{16}$$

$$\mathbf{f}^h = \left\{ \mathbf{f}_i^u \quad \mathbf{f}_i^a \quad \mathbf{f}_i^{b1} \quad \mathbf{f}_i^{b2} \quad \mathbf{f}_i^{b3} \quad \mathbf{f}_i^{b4} \quad \mathbf{f}_i^c \quad \mathbf{f}_i^d \right\}^T \tag{17}$$

$$\mathbf{f}_i^u = \int_{\Omega^e} R_i^T \mathbf{b}\, d\Omega + \int_{\Gamma_t} R_i^T \bar{\mathbf{t}}\, d\Gamma, \; \mathbf{f}_i^a = \int_{\Omega^e} R_i^T H \mathbf{b}\, d\Omega + \int_{\Gamma_t} R_i^T H\, \bar{\mathbf{t}}\, d\Gamma, \; \mathbf{f}_i^{b\alpha} = \int_{\Omega^e} R_i^T \beta_\alpha \mathbf{b}\, d\Omega + \int_{\Gamma_t} R_i^T \beta_\alpha\, \bar{\mathbf{t}}\, d\Gamma$$

$$\mathbf{f}_i^c = \int_{\Omega^e} R_i^T H\, \mathbf{b}\, d\Omega + \int_{\Gamma_t} R_i^T H\, \bar{\mathbf{t}}\, d\Gamma, \; \mathbf{f}_i^d = \int_{\Omega^e} R_i^T \psi(\xi) \mathbf{b}\, d\Omega + \int_{\Gamma_t} R_i^T \psi(\xi)\, \bar{\mathbf{t}}\, d\Gamma \tag{18}$$

where, R_i^T are represents the NURBS basis function. B_i^u, B_i^a, B_i^b, $\mathrm{B}_i^{b\alpha}$, B_i^c and B_i^d are the NURBS basis function derivatives matrices given by:

$$\mathrm{B}_i^u = \begin{bmatrix} R_{i,X_1} & 0 \\ 0 & R_{i,X_2} \\ R_{i,X_2} & R_{i,X_1} \end{bmatrix}_{3\times n_{en}}, \; \mathrm{B}_i^a = \begin{bmatrix} (R_i)_{,X_1} H & 0 \\ 0 & (R_i)_{,X_2} H \\ (R_i)_{,X_2} H & (R_i)_{,X_1} H \end{bmatrix}_{3\times n_{en}}, \; \mathrm{B}_i^b = \begin{bmatrix} \mathrm{B}_i^{b1} & \mathrm{B}_i^{b2} & \mathrm{B}_i^{b3} & \mathrm{B}_i^{b4} \end{bmatrix}$$

$$\mathrm{B}_i^{b\alpha}=\begin{bmatrix}\left(R_i\beta_\alpha\right)_{,X_1} & 0\\ 0 & \left(R_i\beta_\alpha\right)_{,X_2}\\ \left(R_i\beta_\alpha\right)_{,X_2} & \left(R_i\beta_\alpha\right)_{,X_1}\end{bmatrix}_{3\times n_{en}},\ \mathrm{B}_i^{c}=\begin{bmatrix}\left(R_i\right)_{,X_1}\chi & 0\\ 0 & \left(R_i\right)_{,X_2}\chi\\ \left(R_i\right)_{,X_2}\chi & \left(R_i\right)_{,X_1}\chi\end{bmatrix}_{3\times n_{en}},\ \mathrm{B}_i^{c}=\begin{bmatrix}\left(R_i\right)_{,X_1}\chi & 0\\ 0 & \left(R_i\right)_{,X_2}\chi\\ \left(R_i\right)_{,X_2}\chi & \left(R_i\right)_{,X_1}\chi\end{bmatrix}_{3\times n_{en}}$$

$$\mathrm{B}_i^{d}=\begin{bmatrix}\left(R_i\psi\right)_{,X_1} & 0\\ 0 & \left(R_i\psi\right)_{,X_2}\\ \left(R_i\psi\right)_{,X_2} & \left(R_i\psi\right)_{,X_1}\end{bmatrix}_{3\times n_{en}}$$

where, $\alpha=1,2,3,4$

3.5. Computation of Stress Intensity Factor

In the present work, the individual stress intensity factors K_I and K_{II} are obtained using domain form of interaction integral [15].

4. Numerical Simulation and Discussion

In the present work, edge crack problems are simulated using XIGA in the presence of inclusions and holes. In order to check the accuracy and performance of XIGA, the results are compared with XFEM. The order of NURBS function in both parametric directions is taken as 3, and the weight of each control point is taken as unity. First order NURBS with uniform weight is equivalent to the Lagrange finite elements. Uniformly distributed control points are taken for the analysis. The values of SIFs are calculated by interaction integral approach. The material properties [15] used for the simulations are:

Elastic Modulus	$E = 74\,GPa$
Elastic Modulus for Inclusions	$E_I = 20\,GPa$
Poisson Ratio for Material	$\nu = 0.3$
Poisson Ratio for Inclusions	$\nu = 0.3$
Fracture Toughness	$K_{IC} = 1897.36\ N/mm^{3/2}$

The theoretical stress intensity factor can be computed as

$$K_I = C\sigma\sqrt{\pi a},\ C=\left[1.12-0.23\left(\frac{a}{L}\right)+10.6\left(\frac{a}{L}\right)^2-21.7\left(\frac{a}{L}\right)^3+30.4\left(\frac{a}{L}\right)^4\right] \tag{19}$$

4.1. Plate with an edge crack

A plate of size $100\,\mathrm{mm}\times 200\,\mathrm{mm}$ along with a crack length $a=30\,\mathrm{mm}$ is shown in Fig. 1 (a) along with boundary conditions. The control points are taken to be 30×60 for the purpose of simulation. The knot vectors are taken open and uniform without any repetition. The bottom edge of the plate is constrained in the y direction. The plate is subjected to tensile load of $\sigma = 60\ N/mm$ at the top edge. The stress contour plots of σ_{xx} and σ_{yy} are shown in the Fig. 1 (b) and Fig. 2 (a). Table 1 presents the error in mode-I SIF for different control points, and order with the exact solution.

It is observed that as the number of control points and NURBS order are increased, the error obtained is found less as compared to the exact solution. Fig. 2 (b) represents the SIF variation with the crack length. The SIF computed using XIGA gives less error as compared to XFEM.

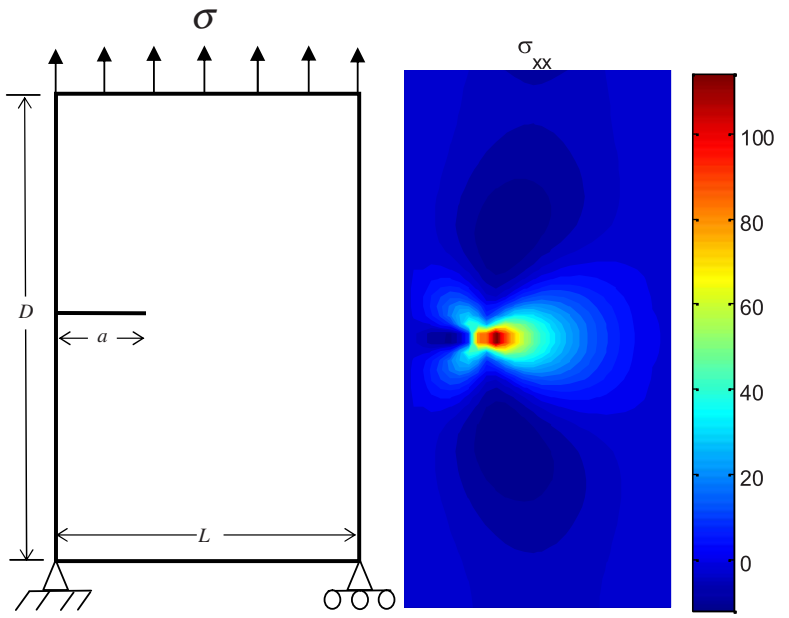

Fig. 1. (a) Edge crack plate along with direction; (b) Stress contour plot (σ_{xx}) for an edge crack plate.

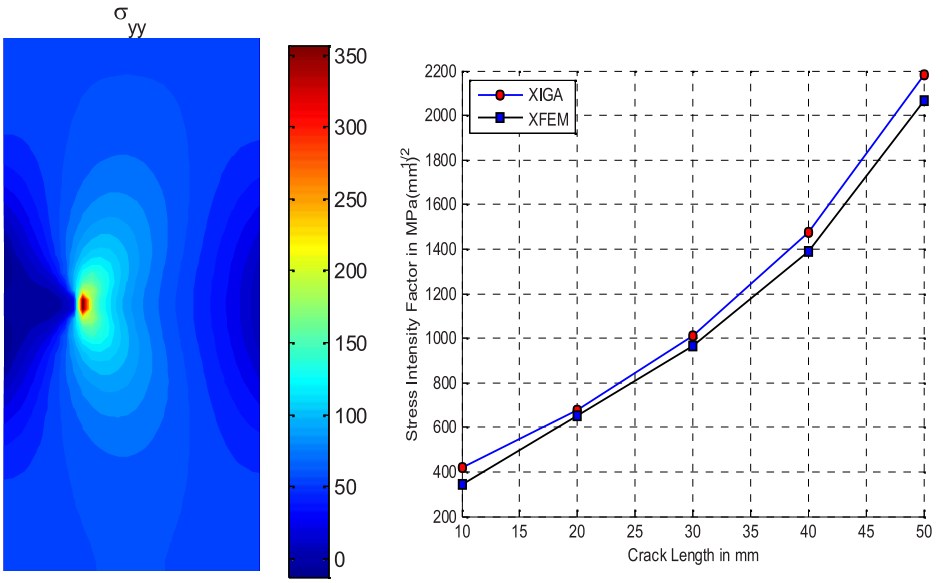

Fig. 2. (a) Stress contour plot (σ_{yy}) for an edge crack plate; (b) SIF variation with crack length for left edge crack.

4.2. Plate with an edge crack and multiple holes

A plate of size $100\,\text{mm} \times 200\,\text{mm}$ along with a crack length of $a = 30\,\text{mm}$, and 16 holes of radii $5\,mm$ are taken for this simulation. The uniformly distributed control points are taken as 60×120. The geometry and boundary conditions are taken similar to the problem 4.1. The σ_{xx}, σ_{yy} and σ_{xy} represents the stress contour plots as shown in Fig. 3 (a), Fig. 3 (b) and Fig. 4 (a) respectively. The values of SIF computed using XIGA are compared with XFEM as shown in Fig. 4 (b).

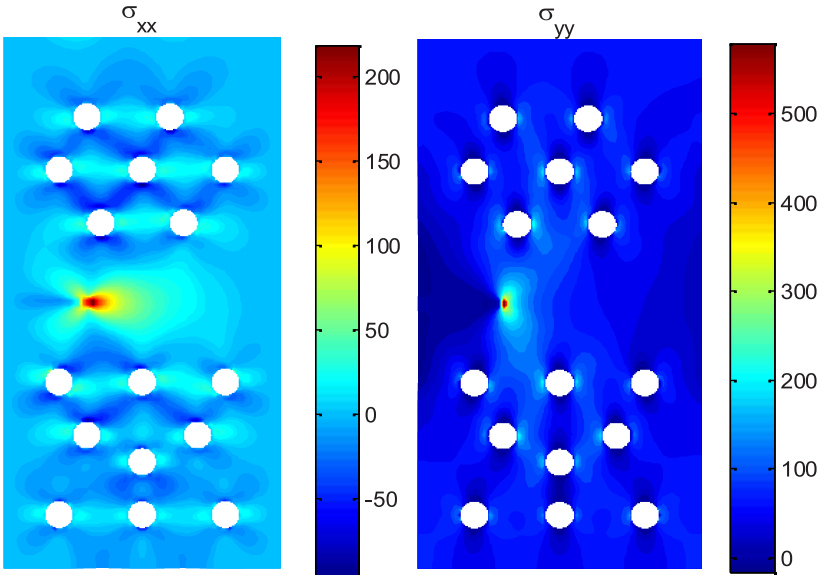

Fig. 3. (a) Contour plot of σ_{xx} for an edge crack with multiple holes; (b) Contour plot of σ_{yy} for an edge crack with multiple holes.

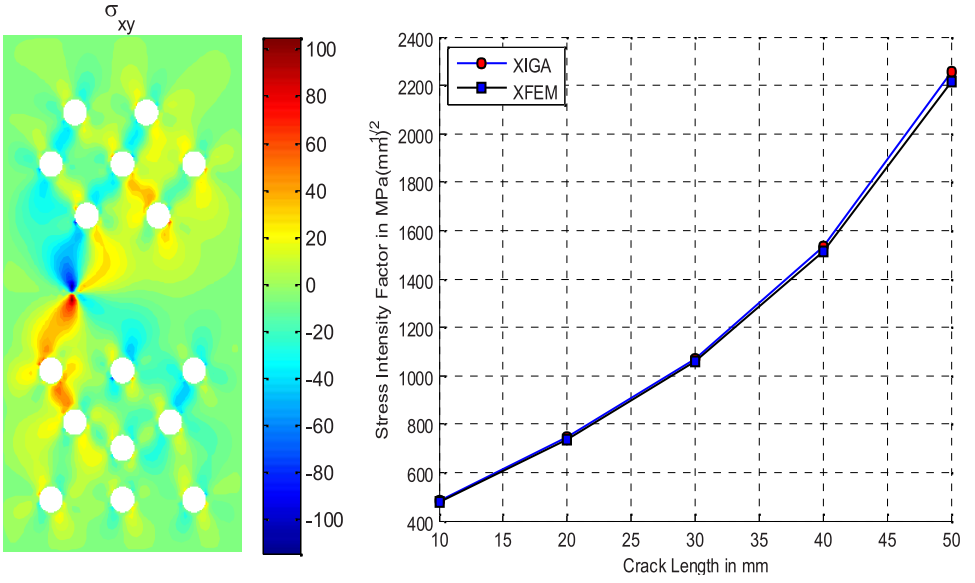

Fig. 4. (a) Contour plot of σ_{xy} for an edge crack with multiple holes; (b) SIF variation with crack length for an edge crack with multiple holes.

4.3. *Plate with an edge crack and multiple inclusions*

A plate of size 100 mm×200 mm along with a crack of length $a = 30$ mm , and 14 inclusions of radii 5 mm are taken for the simulation. The control points are taken as 50×100 . The geometry and boundary conditions are taken as per problem 4.1. The contour plots of σ_{xx}, σ_{yy} and σ_{xy} are shown in Fig. 5 (a), Fig. 5 (b) and Fig. 6 (a) respectively. The SIF values calculated by XIGA are compared with XFEM as shown in Fig. 6 (b).

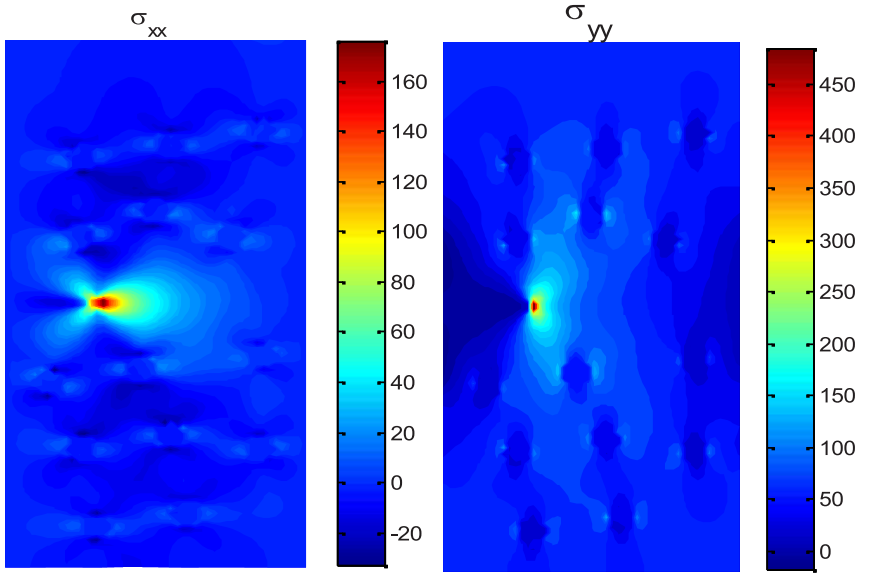

Fig. 5. (a) Contour plot of σ_{xx} for an edge crack with multiple inclusions; (b) Contour plot of σ_{yy} for an edge crack with multiple inclusions.

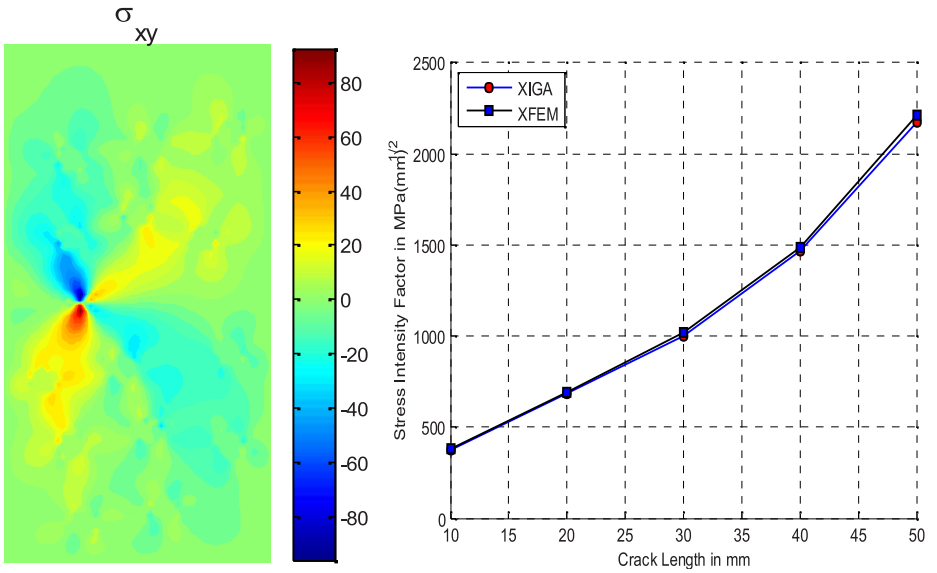

Fig. 6. (a) Contour plot of σ_{xy} for an edge crack; (b) SIF variation with crack length for an edge crack with multiple inclusions.

5. Conclusion

In the present work, XIGA has been used for the simulation of plane crack problems in the presence of holes and inclusions. Both the geometry and solution are defined using NURBS basis function. These simulations show that the accuracy achieved using XIGA with higher order NURBS basis function found more as compared to XFEM. It is also concluded that the presence of discontinuities i.e. holes and inclusions significantly affect the SIFs. The effect of holes on SIF is found more as compared to the inclusions. This work can be extended further for the analysis of fatigue crack in the presences of multiple flaws.

References

[1] Hughes, T. J. R., Cottrell, J. A., Bazilevs, Y., 2005. Isogeometric analysis: CAD, finite elements, NURBS, exact geometry and mesh refinement, Computer Methods in Applied Mechanics and Engineering, 194, pp. 4135-4195.

[2] Verhoosel, C. V., Scott, M. A., Hughes, T. J. R., Borst, R.D, 2011. An isogeometric analysis approach to gradient damage models, International Journal for Numerical Methods in Engineering, 86, pp. 115-134.

[3] Verhoosel, C. V., Scott, M. A., Borst, R. D, Hughes, T. J. R., 2011. An isogeometric approach to cohesive zone modeling, International Journal for Numerical Methods in Engineering, 87, pp. 336-360.

[4] Hassani, B., Khanzadi, M., Tavakkoli, S., Mehdi, 2012. An isogeometrical approach to structural topology optimization by optimality criteria, Structural and multidisciplinary optimization, 45, pp. 223-233.

[5] Temizer, I., Wriggers, P., Hughes, T. J. R., 2011. Contact treatment in isogeometric analysis with NURBS, Computer Methods in Applied Mechanics and Engineering, 200, p. 1100-1112.

[6] Luycker, E. De, Benson, D.J., Belytschko, T., Bazilevs, Y., Hsu, M. C., 2011. X-FEM in isogeometric analysis for linear fracture mechanics, International Journal for Numerical Methods in Engineering, 87, pp. 541-565.

[7] Benson, D. J., Bazilevs, Y., Luycker, E. De, Hsu, M. C., Scott, M. A, Hughes, T. J. R., Belytschko, T., 2010. A generalized finite element formulation for arbitrary basis functions: From isogeometric analysis to XFEM, International Journal for Numerical Methods in Engineering, 83, pp. 765-785.

[8] Ghorashi, S. S, Valizadeh, N., Mohammadi, S., 2011. Extended isogeometric analysis for simulation of stationary and propagating cracks, International Journal for Numerical Methods in Engineering, 89, pp. 1069-1101.

[9] Haasemann, G., Kastner, M., Pruger, S., Ulbricht, V., 2011. Development of a quadratic finite element formulation based on the XFEM and NURBS, International Journal for Numerical Methods in Engineering, 86, pp. 598-617.

[10] Cottrell, J. A, Hughes, T. J. R, and Bazilevs, Y, 2009. Isogeometric Analysis towards Integration of CAD and FEA (first edition), A John and wiley & Sons Ltd, Publications (UK).

[11] Zeid, I., 2007. Mastering CAD/CAM, Tata McGraw-Hill Publishing Company Ltd.

[12] Moes, N., Dolbow, J., Belytschko. T., 1999. A finite element method for crack growth without remeshing, International Journal for Numerical Methods in Engineering, 46, pp. 131–150.

[13] Belytschko, T., Black, T., 1999. Elastic crack growth in finite elements with minimal remeshing, International Journal for Numerical Methods in Engineering, 45, pp. 601–20.